Arabian Journal of Chemistry (2021) **14**, 103240

King Saud University

Arabian Journal of Chemistry

www.ksu.edu.sa
www.sciencedirect.com

ORIGINAL ARTICLE

Quantitative structure-property relationships (QSPR) of valency based topological indices with Covid-19 drugs and application

Jian-Feng Zhong [a], **Abdul Rauf** [b,*], **Muhammad Naeem** [b], **Jafer Rahman** [c], **Adnan Aslam** [d]

[a] *Department of Infectious Diseases, Huzhou Central Hospital, Zhejiang, Huzhou 313000, PR China*
[b] *Department of Mathematics, Air University Multan Campus, Multan, Pakistan*
[c] *Department of Mathematics & Statistics, Hazara University Mansehra, Pakistan*
[d] *Department of Natural Sciences and Humanities, University of Engineering and Technology, Lahore, Pakistan (RCET), Pakistan*

Received 13 April 2021; accepted 27 May 2021
Available online 8 June 2021

KEYWORDS

Ev-degree;
Ve-degree;
Topological indices;
Quantitative Structure-Property Relationships (QSPR);
Camptothecin-Polymer Conjugate IT-101;

05C09;
05C92;
92E10

Abstract The purpose of this analysis is to establish a quantitative structure–property relationship (QSPR) between eV and ve-degree based topological descriptors and measured physicochemical parameters of phytochemicals screened against SARS-CoV-2 $3CL^{pro}$. A computer-based algorithm is developed to compute the eV and ve-degree based topological indices for the considered graphs. Our study revealed that the eV-degree based Zagreb index M^{ev} and ve-degree based first beta Zagreb index $M_1^{\beta ve}$ are two important topological indices that can be useful in the prediction of molecular weight and the topological polar surface area of phytochemicals. Applications to certain anticancer drug (Camptothecin-Polymer Conjugate IT-101) are presented at the end.

1. Introduction

Chemical graph theory is a branch of science which deals with the graphical representation of the chemical structure. In chemistry, the chemical compounds that have the same molecular formula but different structure are called isomers. In chemical graph theory, the vertices represent the atoms and the edges represent the bonds. Chemical graph theory is used in the modeling of the molecular structure of chemical compounds and also to study their chemical and physical properties. Due to its wide-ranging applications in various fields of life such as electrical networks, biological networks, chemistry, computer science and drug designs, it attains much attention of researchers (Hosamani et al., 2017; Li et al., 2021; Shao et al., 2018). Recently, a mixture field of information science, chemistry and mathematics have been developed, the so-called chem-informatics.

Several viral diseases continue to emerge causing serious public health issue. Among these viral diseases severe acute respiratory coronavirus syndrome (SAR-CoV) were reported

* Corresponding author.
E-mail addresses: attari_ab092@yahoo.com, abdul.rauf@aumc.edu.pk (A. Rauf), jaferattari@hu.edu.pk (J. Rahman).

https://doi.org/10.1016/j.arabjc.2021.103240
1878-5352

in 2002 and 2003 and H1N1 influenza in 2009. A fatal respiratory disease as a result of novel coronavirus strain was reported at the end of 2019 (Xu et al., 2020). Soon after that researcher, Chinese health authorities and Centers for Disease Control and Prevention (CDC) had taken swift action against the disease. WHO temporarily named this virus as a novel coronavirus (2019-nCoV) (Ji et al., 2020).

The first complete 2019-nCoV genome sequence was published on 10 January 2020. On 12 February 2020 the WHO classified the 2019-nCoV pathogen permanently as SARS-CoV-2 and coronavirus disease 2019 as COVID-19. This outbreak was officially declares as pandemic on March 11, 2020 by WHO. Typically, after transcription of the genome, betacoronaviruses generate 800 k Da polypeptide. Proteolytic clamping for several proteins is achieved. Proteolytic treatment is mediated by papain-like protease (PL^{pro}) and 3-chymotrypsin-like protease (3CLpro). Potential inhibitors have been identified for SARS-CoV and MERS-CoV $3CL^{pro}$ based on the structure of activity tests and high throughput studies (Ghosh et al., 2005; Kumar et al., 2016; Pillaiyar et al., 2016). This research is therefore carried out to gain structural insights of SARS-CoV-2, $3CL^{pro}$ and to detect powerful natural compounds to battle COVID-19.

The first emergency use (EUA) vaccine for COVID-19 was released by Food and Drug Administration (FDA) On December 11, 2020. WHO listed Pfizer/BioNtech Comirnaty vaccine in Emergency Use Listing (EUL) on December 31, 2020. On February 16, 2021 the SII/Covishield and AstraZeneca/AZD1222 vaccines, on March 12, 2021 the Janssen/Ad26.COV 2.S developed by Johnson & Johnson and on April 30, 2021 the Moderna COVID-19 vaccine (mRNA 1273) was listed in WHO Emergency Use Listing (EUL). On May 7, 2021 the Sinopharm COVID-19 vaccine was listed for EUL and was produced by the China National Biotec Group. Globally, 165,772,430 confirmed COVID-19 cases were registered to the WHO till May 22, 2021 including 3,437,545 deaths. Various clinicians and researchers are focusing on research and production of antivirals using various methods that combine experimental and in silico (Kumar et al., 2016 Jul 1; Mittal et al., 2019; Muralidharan et al., 2020; Nutho et al., 2020; Needle et al., 2015; Pant et al., 2020; Pushpakom et al., 2019; ul Qamar et al., 2020). The SARS-CoV-2 replication cycle can be broken down into three steps: viral RNA replication, viral entry and viral assembly and evacuation from the host cell, as shown in Fig. 1.

The genome sequence of SARS-CoV-2 was found to be very similar to that of SARS-CoV in recent studies. SARS-CoV-2, $3CL^{pro}$-screened phytochemicals as given in Figs. 2–7 are recently published in (ul Qamar et al., 2020) and several researchers are working to find better and productive instruments and medicines to combat diseases.

Topological indices are often characterized by using vertex and edge degree-based concepts and play an important role in theoretical chemistry. The first topological descriptor was put forward by Wiener (1947) and is related with the critical point, boiling points, and density of paraffin. The Randic index was proposed by Randic in 1975 (Randic, 1975) and generalized by Bollobás and Erdös (1998). The first and second Zagreb index was introduced by Gutman and Trinajstic (1972) about forty years ago. The atom-bond connectivity (ABC) index was initi-

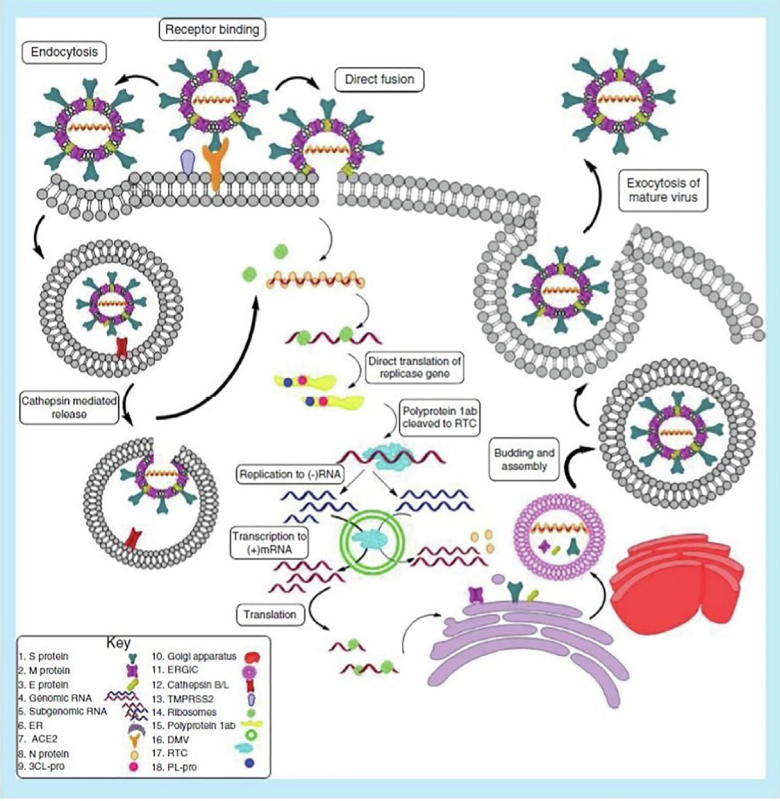

Fig. 1 SARS-COV-19 replication cycle.

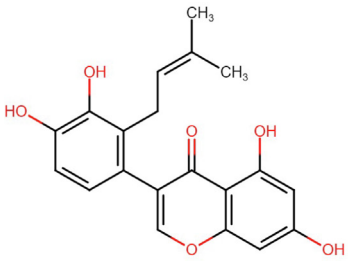

(a) $5,7,3',4' - Tetrahydroxy - 2' - (3,3 - dimethylallyl)isoflavone$

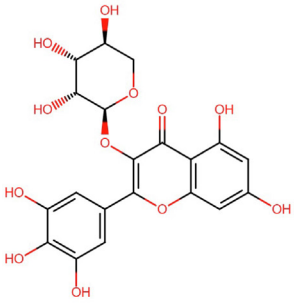

(b) $Myricitrin$

Fig. 2

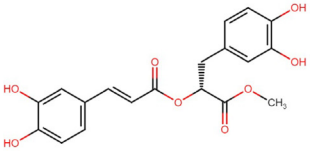

(a) $Methylrosmarinate$

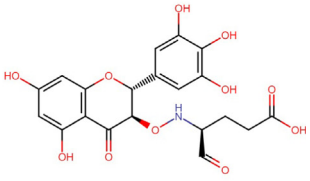

(b) $3,5,7,3',4',5' - hexahydroxyflavanone - 3 - O - beta - D - glucopyranoside$

Fig. 3

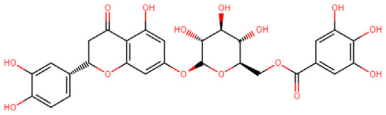

(a) $(2S) - Eriodictyol7 - O - (6'' - O - galloyl) - beta - D - glucopyranoside$

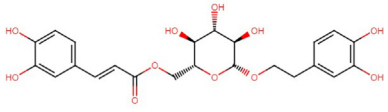

(b) $CalceolariosideB$

Fig. 4

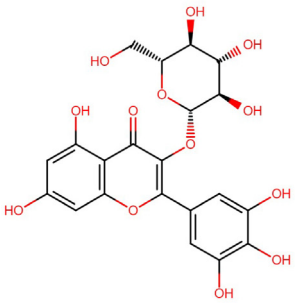

(a) $Myricetin3 - O - beta - D - glucopyranoside$

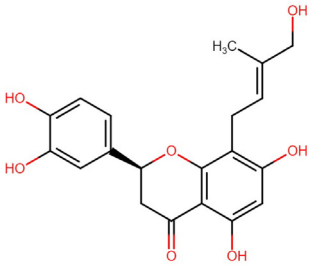

(b) $Licoleafol$

Fig. 5

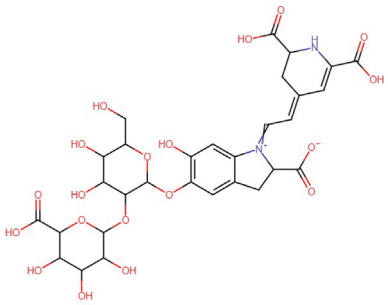

(a) *Amaranthin*

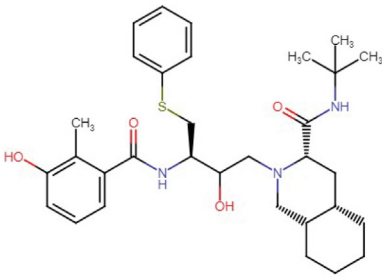

(b) *Nelfinavir*

Fig. 6

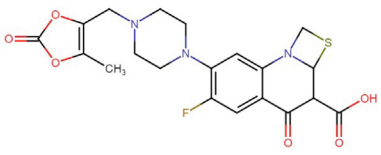

(a) *Prulifloxacin*

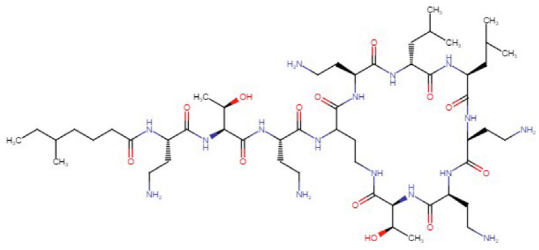

(b) *Colistin*

Fig. 7

ated by Estrada et al. (1998) and geometric-arithmetic index was introduced by Vukičević and Furtula (2009). The ve-degree and eV-degree definitions were introduced by Chellali et al. (2017). The work of Chellali et al. was investigated by Horoldagva (2019) and mathematical concepts were developed. The degree-based ideology transformed into ve-degree, eV-degree, degree-based M-polynomial and NM-polynomials and degree-based entropy. Various researchers calculated the different topological indices for COVID drugs-related structures, for the help of the production of antivirals (Rauf et al., 2021; Al-Ahmadi et al., 2021; Saleh et al., 2021). Liu et al. (2021) studied the structural properties by using bond additive and distance based topological descriptors of antiviral medications for the treatment of COVID 19 such as hydroxychloroquine, chloroquine, lopinavir, theaflavin, ritonavir, remdesivir, nafamostat, umifenovir, bevacizumab, and camostat. Topological indices of chloroquine, theaflavin, remdesivir and hydroxychloroquine are computed in (Mondal et al., 2020). Nandini, G. Kirithiga, et al. have computed topological indices of pandemic trees, corona product of Christmas trees and paths (Nandini et al., 2020). Mondal, Sourav, et al. calculated the multiplicative degree-based indices for some anti-COVID-19 chemicals such as hydroxychloroquine, theaflavin and remdesivir (GS-5734) (Mondal et al., 2020). Wei, Jianxin, et al. calculated the reverse indices for remdesivir (GS-5734) (Wei et al., 2021). Kirmani, Syed Ajaz K., Parvez Ali, and Faizul Azam investigated several antiviral drugs and QSPR was established between topological indices and various physical/-chemical properties of antiviral drugs (Kirmani et al., 2021).

In the QSPR study, the bioactivity of chemical compounds can be predicted by using topological indices. Shirakol et al. (2019) study the QSPR analysis of degree-distance and distance based topological indices for their predicting power. Similarly, Luccic et al. (2001) study the QSPR for novel distance-related indices. Using modified Xu and atom-type-based AI topological indices a QSPR was performed for the prediction of enthalpies of 134 acyclic alkanes by Safa and Yekta (2017). H. Sunilkumar et al. studied the QSPR analysis of degree-based topological indices to characterize the useful topological indices based on their predicting power (Hosamani et al., 2017). For more details on QSPR study of topological indices see (Mondal et al., 2021; Sahoo et al., 2011). The main objective of this paper is to establish a relation between topological descriptors and physical/chemical parameters of phytochemicals that are used for screening against SARS-CoV-2, $3CL^{pro}$ in a quantitative structure–property. In this paper, we have considered five ve and eV-degree based topological indices see (Şahin1 and Ediz, 2018).

Let G be a connected graph with vertex set and edge set denoted by $V(G)$ and $E(G)$ respectively. For any $v \in V(G)$, let $\Lambda(v)$ represent the degree of the vertex $v \in V(G)$ and is the number of edges linked to v. The open neighborhood of the vertex v is the set of all vertices that are adjacent to v. The closed neighborhood of v, denoted by $N[v]$ is defined as the union of v vertex with open neighborhood of v. The eV-degree of any edge $e = uv \in E(G)$, denoted by $\Lambda_{ev}(e)$ is the total number of the vertices of closed neighborhoods of the end vertices of an edge e. The ve-degree of any vertex $v \in V(G)$, denoted by $\Lambda_{ve}(v)$ is the total number of edges which are adjacent to v and the first neighbor of v, i.e., the sum of degrees of all closed neighbourhood vertices of v.

Ev-degree based indices

The indices based on eV-degree, such as the Zagreb index (M^{ev}) and the Randic index (R^{ev}) for any edge $e = uv \in E(G)$ are defined as

$$M^{ev}(G) = \sum_{e \in E} \Lambda_{ev}(e)^2,$$

$$R^{ev}(G) = \sum_{e \in E} \Lambda_{ev}(e)^{-\frac{1}{2}}.$$

Ve-degree based index

For any vertex $v \in V(G)$, the first Zagreb alpha index ($M_1^{\alpha ve}$) based on ve-degree is defined as

$$M_1^{\alpha ve}(G) = \sum_{v \in V} \Lambda_{ve}(v)^2.$$

Ve-degree of end vertices of each edge

The first and second Zagreb beta index denoted by $M_1^{\beta ve}$ and $M_2^{\beta ve}$ respectively of each edge $uv \in E(G)$ based on ve-degree of end vertices are defined as

$$M_1^{\beta ve}(G) = \sum_{uv \in E} (\Lambda_{ve}(u) + \Lambda_{ve}(v)),$$

$$M_2^{\beta ve}(G) = \sum_{uv \in E} (\Lambda_{ve}(u) \times \Lambda_{ve}(v)).$$

The distribution of the sections has the following details, see the procedure detail in Fig. 8. Section 2 describe the schematic computer-based algorithm to calculate the degree vector, ve-degree vector, and eV-degree matrix and the respective topological indices for a given graph through Maple software. The Section 4 describes the quantitative-structure–property analysis (QSPR) of phytochemicals screened against SARS-CoV-23CL^{pro} with the help of eV and ve degree-based topological descriptors. Applications to certain anticancer drug (Camptothecin-Polymer Conjugate IT-101) is presented in Section 5. Section 6 is the numerical results and discussion and Section 7 is conclusion. Section 3 describes an illustrative example to demonstrate the algorithm described in Section 2.

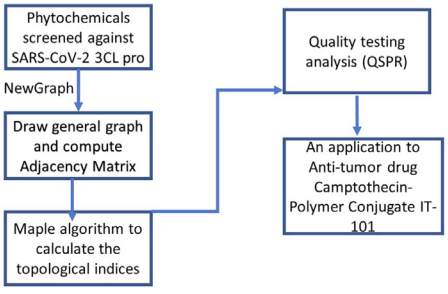

Fig. 8 Working flowchart.

2. Algorithm

1: Start
2: Input: M is adjacency matrix of a Graph.
3: Output: Calculation of Ve-Degree, Ev-degree, Ve-degrees of end vertices of each edge, and the Ev and Ve degree based topological indices.
4: Initialization: E ←No. of edges, V ←No. of vertex, con[E] ←connection matrix, deg[V] ←degree of each vertex, VE←VE-Degree of vertices, deg [VE] ←No. of edges incident to the closed neighborhood vertices, EV←EV-Degree of adjacent vertices, deg [EV] ←the sum of the degree of two adjacent vertices, ver[V] ←Vertex list, count ←1, adj[count] ←adjacent element, Mq [count] ←VE-Degree matrices elements, Mp[count] ←EV-Degree matrices elements.
5: loop a = 1 to V
6: For each vertex from the array ver[V].
7: loop b = 1 to E
8: count corresponding vertex from the matrix con[E].
9: b++
10: end loop
11: deg[V] = count.
12: loop c = 1 to count
13: adj[count] = store corresponding vertex.
14: c++
15: end loop
16: loop d = 1 to deg[V]count
17: Multiply Matrix M and adj[count]
18: Store the result of the above as VE
19: d++
20: end loop
21: loop e = 1 to V
22: loop f = 1 to V
23: Summation of deg[V][e] with deg[V][f] and multiply by (i,j) th element of Adjacency Matrix.
24: Store the result of the above as EV
25: f++
26: end loop
27: e++
28: end loop
29: end loop
30: loop g = 1 to VE
31: For each vertex from the array VE
32: loop h = 1 to VE
33: count vertex from the matrix for VE
34: end loop
35: deg[VE]=count
36: loop k = 1 to count
37: Mq[count]= store vertices for VE.
38: k++
39: end loop
40: end loop
41: loop l = 1 to EV
42: For each adjacent vertex from the array EV
43: loop m = 1 to EV
44: count corresponding vertices from the array EV

(*continued on next page*)

```
45:          m++
46:      end loop
47:      deg[EV]=count
48:      loop n = 1 to count
49:          Mp[count]=store EV
50:          n++
51:      end loop
52: end loop
53: loop o = 1 to count
54:      Calculate the VE-Degree based first Zagreb Alpha index.
55: end loop
56: loop p = 1 to count
57:      Calculate the EV-Degree based Zagreb Index and Randic
Index.
58: end loop
59: loop q = 1 to E
60:      Calculate the End Vertices Ve degree for each Edge, the
first and second Zagreb beta index based on the ve-degree of end
vertices of each edge, the first Zagreb alpha index based on ve-
degree, the Zagreb and Randic index based on eV-degree.
61: end loop
62: end
```

a, b, c, d, e, f, g, h, k, l, m, n, o, p and q all are variables whose data type is an integer. We are using these variables for iterating through the matrix using indices in a loop.

3. Illustrative example on Algorithm

We calculated the degree vector, ve-degree vector, and eV-degree matrix and the respective topological indices for a given graph through the Maple algorithm given above. For this we consider the example of starphene graph (S) for $n = 2, m = 2$ and $l = 2$, see Fig. 9. First, we write the adjacency matrix (A) of the graph S in MAPLE. We get the adjacency matrix A by newGraph software (procedure mentioned in (Hayat and Khan, 2021)). As there are 18 vertices in the graph, the order of the A will be 18–18 and from figure it is clear that the graph S has 21 edges.

$$A = \begin{bmatrix}
0&1&0&0&0&0&0&0&0&0&0&0&0&0&0&0&0&1\\
1&0&1&0&0&0&0&0&0&0&0&0&0&0&0&0&0&0\\
0&1&0&1&0&0&0&0&0&0&0&0&0&0&0&0&0&0\\
0&0&1&0&1&0&0&0&0&0&0&0&0&0&0&0&1&0\\
0&0&0&1&0&1&0&0&0&1&0&0&0&0&0&0&0&0\\
0&0&0&0&1&0&1&0&0&0&0&0&0&0&0&0&0&0\\
0&0&0&0&0&1&0&1&0&0&0&0&0&0&0&0&0&0\\
0&0&0&0&0&0&1&0&1&0&0&0&0&0&0&0&0&0\\
0&0&0&0&0&0&0&1&0&1&0&0&0&0&0&0&0&0\\
0&0&0&0&1&0&0&0&1&0&1&0&0&0&0&0&0&0\\
0&0&0&0&0&0&0&0&0&1&0&1&0&0&0&1&0&0\\
0&0&0&0&0&0&0&0&0&0&1&0&1&0&0&0&0&0\\
0&0&0&0&0&0&0&0&0&0&0&1&0&1&0&0&0&0\\
0&0&0&0&0&0&0&0&0&0&0&0&1&0&1&0&0&0\\
0&0&0&0&0&0&0&0&0&0&0&0&0&1&0&1&0&0\\
0&0&0&0&0&0&0&0&0&0&1&0&0&0&1&0&1&0\\
0&0&0&1&0&0&0&0&0&0&0&0&0&0&0&1&0&1\\
1&0&0&0&0&0&0&0&0&0&0&0&0&0&0&0&1&0
\end{bmatrix}$$

Now, with the help of the adjacency matrix we can calculate the degree of vertices, Ve-degree and Ev-degree. The degree of a vertex can be obtained by adding the entries of the corresponding row and we get the degree sequence of starphene graph S in the form of row matrix B.

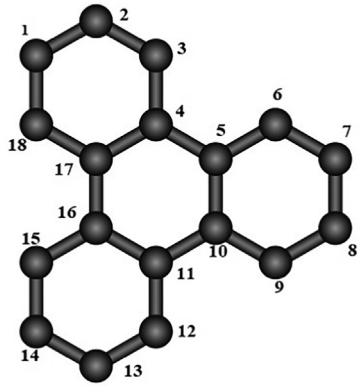

Fig. 9 Molecular structure of starphene for $n = 2, m = 2$ and $l = 3$.

$$B = [2,2,2,3,3,2,2,2,2,3,3,2,2,2,2,3,3,2]$$

Note that the degree sequence is according to the vertices labeled in Fig. 9. For Ve-degree of vertices, we multiplied the adjacency matrix A and B. The column matrix AB represent the Ve-degree of vertices.

$$AB = [4,4,5,8,8,5,4,4,5,8,8,5,4,4,5,8,8,5]$$

Let A_{ij} denote the entry in the i-th row and j-th column of adjacency matrix A and B_i denoted the i-th entry of row matrix B. We multiply the entry A_{ij} of adjacency matrix A with the entry $B_i + B_j$ to obtain a entry L_{ij} of matrix L. The nonzero entries in the upper/lower triangular form of this matrix L give the Ev-degree list of the given graph.

$$L = \begin{bmatrix}
0&4&0&0&0&0&0&0&0&0&0&0&0&0&0&0&0&4\\
0&0&4&0&0&0&0&0&0&0&0&0&0&0&0&0&0&0\\
0&0&0&5&0&0&0&0&0&0&0&0&0&0&0&0&0&0\\
0&0&0&0&6&0&0&0&0&0&0&0&0&0&0&0&6&0\\
0&0&0&0&0&5&0&0&0&6&0&0&0&0&0&0&0&0\\
0&0&0&0&0&0&4&0&0&0&0&0&0&0&0&0&0&0\\
0&0&0&0&0&0&0&4&0&0&0&0&0&0&0&0&0&0\\
0&0&0&0&0&0&0&0&4&0&0&0&0&0&0&0&0&0\\
0&0&0&0&0&0&0&0&0&5&0&0&0&0&0&0&0&0\\
0&0&0&0&0&0&0&0&0&0&6&0&0&0&0&0&0&0\\
0&0&0&0&0&0&0&0&0&0&0&5&0&0&0&6&0&0\\
0&0&0&0&0&0&0&0&0&0&0&0&4&0&0&0&0&0\\
0&0&0&0&0&0&0&0&0&0&0&0&0&4&0&0&0&0\\
0&0&0&0&0&0&0&0&0&0&0&0&0&0&4&0&0&0\\
0&0&0&0&0&0&0&0&0&0&0&0&0&0&0&5&0&0\\
0&0&0&0&0&0&0&0&0&0&0&0&0&0&0&0&6&0\\
0&0&0&0&0&0&0&0&0&0&0&0&0&0&0&0&0&5\\
0&0&0&0&0&0&0&0&0&0&0&0&0&0&0&0&0&0
\end{bmatrix}$$

We use separate formula commands against each index. The calculated values of the topological indices for the given graph are

$$\begin{aligned}
M^{ev}(S) &= 510\\
M_1^{zve}(S) &= 630\\
M_1^{\beta ve}(S) &= 252\\
M_2^{\beta ve}(S) &= 792\\
R^{ev}(S) &= \tfrac{3\sqrt{5}}{5} + \tfrac{3\sqrt{10}}{10} + \tfrac{3}{2}
\end{aligned}$$

4. Quality testing analysis

In this section, we study the QSPR of phytochemicals that are used for screening against SARS- CoV-23CL^{pro} using eV and ve degree-based topological descriptors. The productivity of the topological indices listed above was checked using the phytochemical data set contained in (Balaban, 1982) and https://pubchem.ncbi.nlm.nih.gov/. The data contains the information of the following variables: binding affinity, molecular weight, docking score and topological polar surface. IDs of phytochemicals are mentioned in Table 1 and their properties in Table 2. We could not found topological polar surface and molecular weight of NPACT00105. Therefore, we do not include NPACT00105 for QSPR. Ve-degree and eV-degree based topological indices are presented in Table 3. Table 4 shows the results of correlation coefficients between each pair of variables. We note that all the results are highly significant at 1% level of significance. This shows that there exists a strong positive linear bivariate relationship in the group of variables. The same extent of correlation is depicted in the Figs. (10) and (11). The table suggests that molecular weight (MW) and topological polar surface (TPS) depend on other indices such as $M^{ev}, R^{ev}, M_1^{zve}, M_1^{\beta ve}$ and $M_2^{\beta ve}$. Keeping in mind the above relationships, we consider the following linear regression model for prediction analyses. (see Fig. 12)

$$P = a + bTI$$

Where P consists of either MW or TPS and TI denotes a predictor in the list ($M^{ev}, R^{ev}, M_1^{zve}, M_1^{\beta ve}, M_2^{\beta ve}$).

Based on the data in Table 3 with 12 observations in each variable, we have the following estimated regression equations which can be used to predict molecular weight for a given value of any index $M^{ev}, R^{ev}, M_1^{zve}, M_1^{\beta ve}$ and $M_2^{\beta ve}$.

Table 1 Phytochemical Name and PubChem IDs.

PhytochemicalName	*PubChemIDs*
$5,7,3',4' - Tetrahydroxy - 2' - (3,3 - dimethylallyl)isoflavone$	1610052
Myricitrin	5281673
Methylrosmarinate	6479915
$3,5,7,3',4',5' - hexahydroxyflavanone - 3 - O - beta - D - glucopyranoside$	NPACT00105
$(2S) - Eriodictyol7 - O - (6'' - O - galloyl) - beta - D - glucopyranoside$	10930068
CalceolariosideB	5273567
$Myricetin3 - O - beta - D - glucopyranoside$	5318606
Licoleafol	1111196
Amaranthin	6123095
Nelfinavir	64143
Prulifloxacin	65947
Colistin	5311054

Table 2 Properties of phytochemical.

PubChem IDs	*Docking Score*	*Binding Affinity*	*Molecular Weight*	*Tolpological Polar Surface*
1610052	−16.35	−29.57	354.40	107
5281673	−15.64	−22.13	464.40	207
6479915	−15.44	−20.62	374.30	134
NPACT00105	−14.42	−19.10	0.00	00
10930068	−14.41	−19.47	602.50	253
5273567	−14.36	−19.87	478.40	186
5318606	−13.70	−18.42	480.40	227
1111196	−13.63	−19.64	372.40	127
6123095	−12.67	−18.14	726.60	346
64143	−12.20	−17.31	567.80	127
65947	−11.32	−15.40	461.50	125
5311054	−13.73	−18.57	1155.40	491

Table 3 Ve-degree and Ev-degree based Topological Indices.

PubChem IDs	M^{ev}	R^{ev}	$M_1^{\alpha ve}$	$M_1^{\beta ve}$	M_2^{ve}
11610052	1306	29.5225	1532	590	1954
5281673	1664	50.0469	2005	766	2699
6479915	1270	20.7257	1505	578	1855
NPACT00105	1532	22.9972	1857	700	2359
10930068	2190	32.5014	2110	1226	4862
5273567	1802	27.2264	2152	816	2784
5318606	1736	24.5579	1902	726	2404
11111496	1450	18.4823	1748	591	2197
6123095	2909	41.731	3483	1284	4822
64143	3000	37.4362	3602	1139	4801
605947	1804	24.0714	2133	804	2943
5311054	6116	76.8146	7152	2638	9107

Table 4 Correlation matrix.

	MW	TPS	M^{ev}	R^{ev}	$M_1^{\alpha ve}$	$M_1^{\beta ve}$	$M_2^{\beta ve}$
MW	1.000	0.934	0.974	0.873	0.961	0.987	0.970
TPS		1.000	0.846	0.816	0.826	0.886	0.847
M^{ev}			1.000	0.880	0.996	0.986	0.975
R^{ev}				1.000	0.880	0.883	0.861
$M_1^{\alpha ve}$					1.000	0.969	0.955
$M_1^{\beta ve}$						1.000	0.989
$M_2^{\beta ve}$							1.000

$$MW = a + bX$$
$$MW = 189.809 + 0.159M^{ev}$$
$$MW = 148.351 + 11.687R^{ev}$$
$$MW = 198.166 + 0.133M_1^{\alpha ve}$$
$$MW = 171.654 + 0.377M_1^{\beta ve}$$
$$MW = 178.179 + 0.103M_2^{\beta ve}$$

Table 5 gives the results for correlation coefficient (r), coefficient of determination (R^2), F-statistic (F) and standard error of the estimates (s) for simple linear regression models between MW and various predictors. The results exhibit that the estimated model of MW on $M_1^{\beta ve}$ consists of highest coefficient of determination and F-value ($R^2 = 0.9742$, $F = 375.812$) and least standard error ($s = 37.0609$). This means that the model is highly significant. The only index $M_1^{\beta ve}$ has a high influence on MW and the observed values fall closer to the fitted line. Thus, $M_1^{\beta ve}$ is the best predictor of molecular weight. Similarly, M^{ev} predicts molecular weight better than others after $M_1^{\beta ve}$. A priority list of indices according to their performance is given in Table 7.

Following are the estimated models for predicting topological polar surface for a given value of any index $M^{ev}, R^{ev}, M_1^{\alpha ve}, M_1^{\beta ve}$ and $M_2^{\beta ve}$. The estimation results are based on the data in Table 3 with 12 observations in each variable.

$$TPS = 53.422 + 0.070M^{ev}$$
$$TPS = 21.712 + 5.572R^{ev}$$
$$TPS = 58.694 + 0.058M_1^{\alpha ve}$$
$$TPS = 39.863 + 0.172M_1^{\beta ve}$$
$$TPS = 47.565 + 0.046M_2^{\beta ve}$$

Table 6 gives the results of various statistics for bivariate regression equations of TPS on either of $M^{ev}, R^{ev}, M_1^{\alpha ve}, M_1^{\beta ve}$ and $M_2^{\beta ve}$. We observe that the estimated regression of TPS on $M_1^{\beta ve}$ possesses highest values of coefficient of determination and F-statistic ($R^2 = 0.7850$, $F = 36.529$) and least value of standard error of regression ($s = 54.4280$). The results reveal that the regression model (TPS on $M_1^{\beta ve}$) is highly significant. TPS is highly determined by only $M_1^{\beta ve}$ and the estimated line fits the observations closer than other lines. Hence, $M_1^{\beta ve}$ seems to the best predictor of topological polar surface as well. The hierarchical order of the indices according to their performance is shown in Table 7.

Based on correlation and regression analyses, we may conclude that both molecular weight and the topological polar surface can be predicted well by the indices in the order mentioned in Table 7. However, these indices cannot determine the other variables well such as docking scores (DS) and binding affinity (BA). Table 8 shows the results of the bivariate corre-

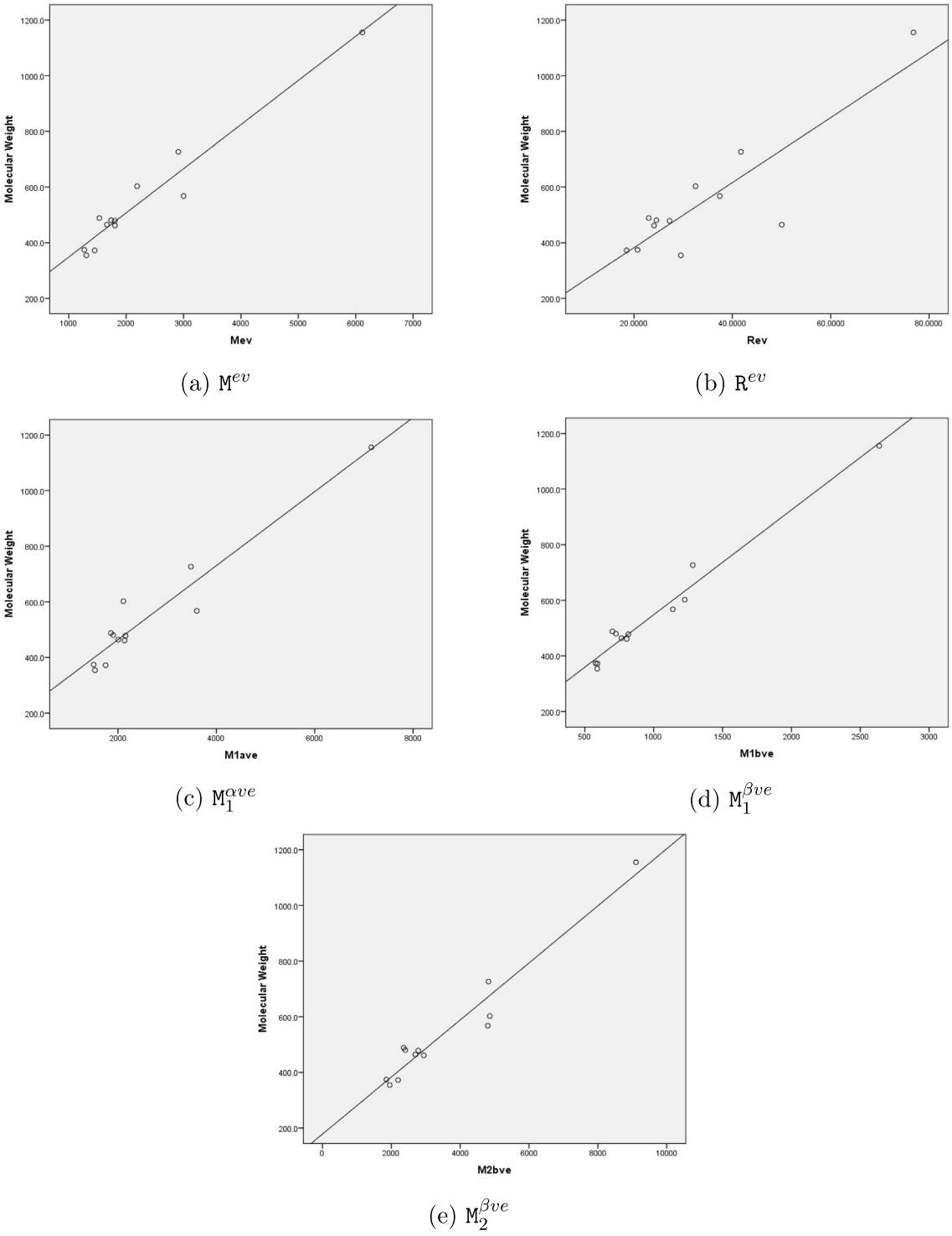

(a) $\mathtt{M}^{ev}$ (b) $\mathtt{R}^{ev}$

(c) $\mathtt{M}_1^{\alpha ve}$ (d) $\mathtt{M}_1^{\beta ve}$

(e) $\mathtt{M}_2^{\beta ve}$

Fig. 10 Graphical representation of linear regression model between topological indices and molecular weight.

lation coefficient which are all insignificant. This means that DS and BA are not linearly correlated with all the indices M^{ev}, R^{ev} , $M_1^{\alpha ve}, M_1^{\beta ve}$ and $M_2^{\beta ve}$. Thus, linear regression cannot model their relationship.

5. Camptothecin-Polymer Conjugate IT-101

Camptothecin (CA) is an alkaloid with a unique anticancer function, operates with a vital and unique mechanism of

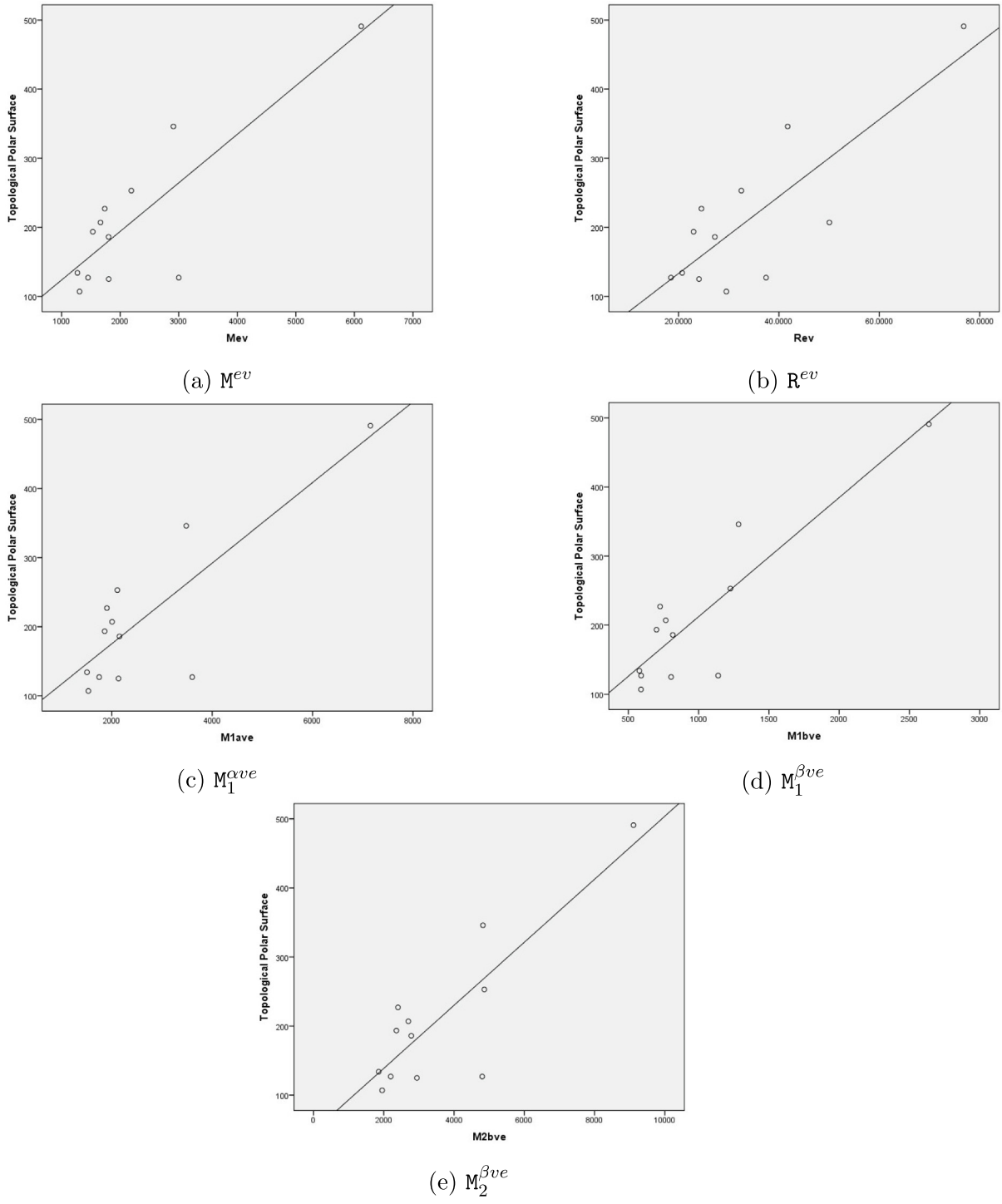

Fig. 11 Graphical representation of linear regression model between topological indices and topological polar surface.

the action to target the topoisomerase (I) nuclear enzyme. The development of a large range of tumors is inhibited by CA. IT-101 is a conjugate of camptothecin with a cyclodextrin-based polymer (Schluep et al., 2006). Topoisomerase I is affected by a drug known as Camptothecin, derived from the Chinese tree, that allows the DNA cleavage, but it inhibits the subsequent ligation and breaks the DNA chain. The systemic application of the camptothecin has some limitations due to severe toxicity. Camptothecin shows potent in vitro anti-glioma activity, making it another common polymer delivery candidate. In the 9L gliosarcoma rat model, sodium salt of camptothecin loaded into 50 percent polymers was checked and resulted in a substantial survival increase (Thomas et al., 2004). The median survival with camptothecin polymers was nineteen days in the model of control rats and up to 120 days. Compared with controls, when we

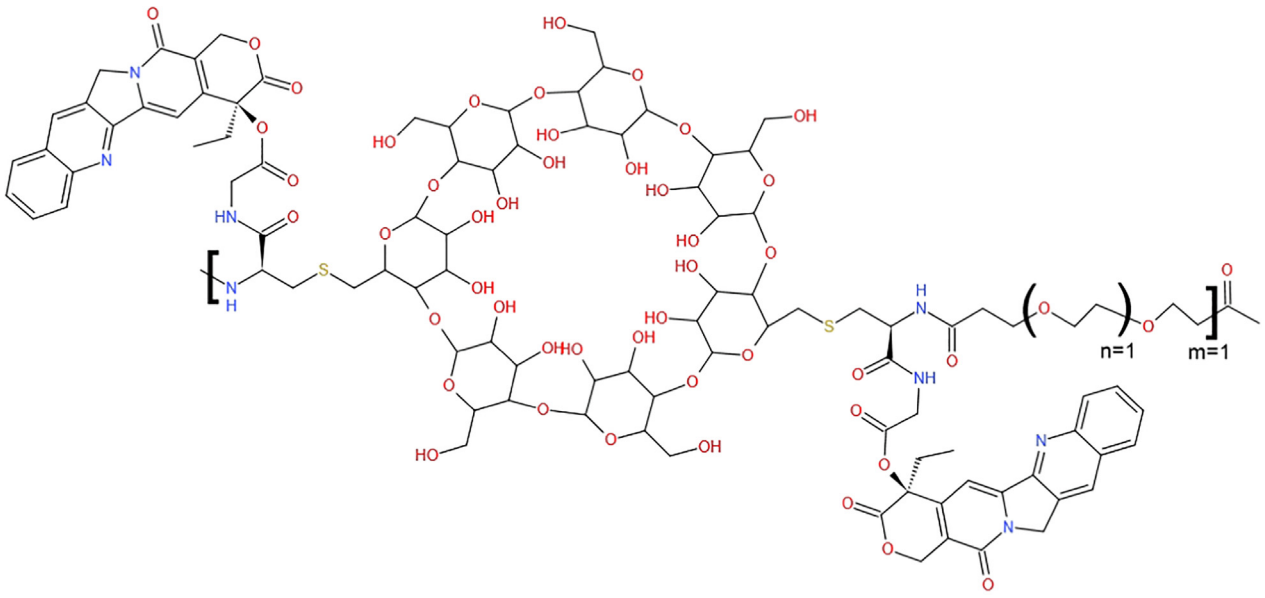

Fig. 12 Molecular Structure of IT-101. The components of the parentpolymer are polyethylene glycol and β-cyclodextrin. Camptothecin is attached to the polymer via a single glycine amino acid linker, where n and m represent the number of repeating units of ethylene glycol and cyclodextrin-based polymer-camptothecin in the polymer-camptothecin conjugate respectively.

Table 5 Performance measures.

X	r	R^2	F	s
M^{ev}	0.9737	0.9481	182.3956	52.4815
R^{ev}	0.8729	0.762	31.996	112.3313
$M_1^{\alpha ve}$	0.9606	0.9228	119.339	64.0086
$M_1^{\beta ve}$	0.987	0.9742	375.812	37.0609
$M_2^{\beta ve}$	0.9705	0.9419	161.769	55.5432

Table 6 Performance measures.

X	r	R^2	F	s
M^{ev}	0.8458	0.7154	25.140	62.6308
R^{ev}	0.8160	0.6659	19.925	67.8686
$M_1^{\alpha ve}$	0.8259	0.6821	21.457	66.1960
$M_1^{\beta ve}$	0.8860	0.7850	36.529	54.4280
$M_2^{\beta ve}$	0.8467	0.7169	25.324	62.4670

Table 7 Correlation coefficient and F Values.

Index	Priority-wise Position
$M_1^{\beta ve}$	1
M^{ev}	2
$M_2^{\beta ve}$	3
$M_1^{\alpha ve}$	4
R^{ev}	5

used direct intratumoral injection of our drug camptothecin without polymer then it showed no betterment in the survival (Liu et al., 2000). Studies integrating camptothecin into 50% polymers for the treatment of 9L gliosarcoma in the rats. It gives protection and efficacy with the survival of 69 days in animals that were treated with the drug camptothecin. Under similar conditions, polymer administration of intracranial camptothecin showed a substantial betterment in survival as compared with the alone camptothecin (Schultz, 1973). In

Table 8 Insignificant correlations.

	DS	BA	M^{ev}	R^{ev}	$M_1^{\alpha ve}$	$M_1^{\beta ve}$	$M_2^{\beta ve}$
DS	1.000	0.840	0.311	0.015	0.322	0.257	0.325
BA		1.000	0.306	0.039	0.304	0.285	0.329

Table 9 The edges eV-degree of Camptothecin-Polymer Conjugate IT-101.

$(\Lambda(u), \Lambda(v))$	$\Lambda_{ev}(e)$	**Frequency**
$E_{(1,\ 2)}$	3	$19m$
$E_{(1,\ 3)}$	4	$25m+1$
$E_{(1,\ 4)}$	5	$4mn+85m+6$
$E_{(2,\ 3)}$	5	$8m$
$E_{(2,\ 4)}$	6	$mn+60m$
$E_{(3,\ 3)}$	6	$35m$
$E_{(3,\ 4)}$	7	$20m+2$
$E_{(4,\ 4)}$	8	$mn+43m$

our work, we compute five ve-degree and eV-degree based topological indices (Chen et al., 2021) of Camptothecin-Polymer Conjugate IT-101. The vertex set of Camptothecin-Polymer Conjugate IT-101 can be partitioned in four set based on the degree of vertices. There are $4mn+129m+7$ vertices of degree $1, mn+33m$ vertices of degree $2, 43m+1$ vertices of degree 3 and $2mn+62m+2$ vertices of degree 4. Similarly, the Edge partition $E_{(i,\ j)}$ of IT-101 based on the degree of end vertices i and j of an edge $e=ij$ is as follows; $E_{(1,\ 2)}$ with $19m$ edges, $E_{(1,\ 3)}$ with $25m+1$ edges, $E_{(1,\ 4)}$ with $4mn+85m+6$ edges, $E_{(2,\ 3)}$ with $8m$ edges, $E_{(2,\ 4)}$ with $mn+60m$ edges, $E_{(3,\ 3)}$ with $35m$ edges, $E_{(3,\ 4)}$ with $20m+2$ edges and $E_{(4,\ 4)}$ with $mn+43m$ edges.

Theorem 1. Let H be a molecular graph of Camptothecin-Polymer Conjugate IT-101 structure, then eV-degrees based Zagreb index and eV-degree based Randic index are given by,

(a) $M^{ev}(H) = 200mn + 10048m + 264.$

(b) $R^{ev}(H) = (\frac{4}{\sqrt{5}}+\frac{1}{\sqrt{6}}+\frac{1}{\sqrt{8}})mn+ (\frac{19}{\sqrt{3}}+\frac{25}{\sqrt{4}}+\frac{85}{\sqrt{5}}+\frac{8}{\sqrt{5}}+\frac{60}{\sqrt{6}}+\frac{35}{\sqrt{6}}+\frac{20}{\sqrt{7}}+\frac{43}{\sqrt{8}})m. (\frac{1}{\sqrt{4}}+\frac{6}{\sqrt{5}}+\frac{2}{\sqrt{7}}).$

Proof. By using the definition, we have calculated the eV-degree of the each edge partition as shown in Table 1.

From Table 9, we can calculate the eV-degree based indices such as: (see Table 10)

(a) The Zagreb index

$$M^{ev}(H) = \sum_{e\in E(H)} \Lambda_{ev}(e)^2,$$

$$\begin{aligned} M^{ev}(H) &= (3)^2|E_{(1,2)}| + (4)^2|E_{(1,3)}| + (5)^2|E_{(1,4)}| + (5)^2|E_{(2,3)}| + (6)^2|E_{(2,4)}| \\ &+ (6)^2|E_{(3,3)}| + (7)^2|E_{(3,4)}| + (8)^2|E_{(4,4)}| \\ &= 200mn + 10048m + 264. \end{aligned}$$

Table 10 The vertex ve-degree of Camptothecin-Polymer Conjugate IT-101

$\Lambda(u)$	$\Lambda_{ve}(u)$	**Frequency**
1	2	$19m$
1	3	$25m+1$
1	4	$4mn+85m+6$
2	5	$19m$
2	6	$2m$
2	7	$4m$
2	8	$mn+8m$
3	7	$18m$
3	8	$12m$
3	9	$5m+1$
3	10	$8m$
4	6	2
4	7	$4m$
4	8	$2mn+15m$
4	9	$9m$
4	10	$2m$
4	11	$30m$
4	12	$2m$

(b) The Randic index

$$R^{ev}(H) = \sum_{e\in E(H)} \Lambda_{ev}(e)^{-\frac{1}{2}},$$

$$\begin{aligned} R^{ev}(H) &= (3)^{-\frac{1}{2}}|E_{(1,2)}| + (4)^{-\frac{1}{2}}|E_{(1,3)}| + (5)^{-\frac{1}{2}}|E_{(1,4)}| + (5)^{-\frac{1}{2}}|E_{(2,3)}| + (6)^{-\frac{1}{2}}|E_{(2,4)}| \\ &+ (6)^{-\frac{1}{2}}|E_{(3,3)}| + (7)^{-\frac{1}{2}}|E_{(3,4)}| + (8)^{-\frac{1}{2}}|E_{(4,4)}| \\ &= (\tfrac{4}{\sqrt{5}}+\tfrac{1}{\sqrt{6}}+\tfrac{1}{\sqrt{8}})mn + (\tfrac{19}{\sqrt{3}}+\tfrac{25}{\sqrt{4}}+\tfrac{85}{\sqrt{5}}+\tfrac{8}{\sqrt{5}}+\tfrac{60}{\sqrt{6}}+\tfrac{35}{\sqrt{6}}+\tfrac{20}{\sqrt{7}}+\tfrac{43}{\sqrt{8}})m \\ &+ (\tfrac{1}{\sqrt{4}}+\tfrac{6}{\sqrt{5}}+\tfrac{2}{\sqrt{7}}). \end{aligned}$$

Theorem 2. Let H be a molecular graph of Camptothecin-Polymer Conjugate IT-101 structure, then vertex ve-degree based first Zagreb α-index is

Table 11 Ve-degree of end vertices of each edge of Camptothecin-Polymer Conjugate IT-101

Edge	$(\Lambda_{ve}(u), \Lambda_{ve}(v))$	Frequency
E_1^*	(2, 5)	$19m$
E_2^*	(3, 7)	$18m$
E_3^*	(3, 8)	$6m$
E_4^*	(3, 9)	$m+1$
E_5^*	(4, 6)	6
E_6^*	(4, 7)	$10m$
E_7^*	(4, 8)	$4mn+30m$
E_8^*	(4, 9)	$11m$
E_9^*	(4, 10)	$4m$
E_{10}^*	(4, 11)	$30m$
E_{11}^*	(6, 8)	$4m$
E_{12}^*	(7, 7)	$4m$
E_{13}^*	(5, 8)	$5m$
E_{14}^*	(5, 11)	$14m$
E_{15}^*	(7, 7)	$4m$
E_{16}^*	(7, 12)	$2m$
E_{17}^*	(8, 8)	$mn+7m$
E_{18}^*	(8, 9)	$14m$
E_{19}^*	(8, 11)	$14m$
E_{20}^*	(7, 7)	$6m$
E_{21}^*	(7, 8)	$2m$
E_{22}^*	(7, 9)	$6m$
E_{23}^*	(7, 10)	$8m$
E_{24}^*	(8, 8)	$3m$
E_{25}^*	(8, 9)	$4m$
E_{26}^*	(8, 10)	$2m$
E_{27}^*	(9, 10)	$2m$
E_{28}^*	(10, 10)	$2m$
E_{29}^*	(7, 8)	$2m$
E_{30}^*	(7, 12)	$2m$
E_{31}^*	(8, 8)	$2m$
E_{32}^*	(8, 9)	m
E_{33}^*	(10, 8)	$4m$
E_{34}^*	(8, 11)	$3m$
E_{35}^*	(9, 6)	$m+1$
E_{36}^*	(9, 11)	m
E_{37}^*	(10, 7)	$2m$
E_{38}^*	(10, 12)	$2m$
E_{39}^*	(7, 10)	$2m$
E_{40}^*	(8, 8)	mn
E_{41}^*	(8, 9)	$2m$
E_{42}^*	(8, 11)	$9m$
E_{43}^*	(10, 12)	$2m$
E_{44}^*	(11, 11)	$21m$
E_{45}^*	(9, 11)	$7m$
E_{46}^*	(9, 9)	1

$$M_1^{\alpha ve}(H) = 256mn + 11774m + 258.$$

Proof. By using the definition, the ve-degrees of the vertices are computed. This computation is presented Table 2.

By using the above table, we have a first ve-degree based Zagreb α-index.

$$\begin{aligned}
M_1^{\alpha ve}(H) &= \sum_{v\in V(H)} \Lambda_{ve}(v)^2 \\
M_1^{\alpha ve}(H) &= (2)^2(19m) + (3)^2(25m+1) + (4)^2(4mn+85m+6) + (5)^2(19m) + (6)^2(2m) + (7)^2(4m) \\
&+ +(8)^2(mn+8m) + (7)^2(18m) + (8)^2(12m) + (9)^2(5m+1) + (10)^2(8m) \\
&+ (6)^2(2) + (7)^2(4m) + (8)^2(2mn+15m) + (9)^2(9m) + (10)^2(2m) \\
&+ (11)^2(30m) + (12)^2(2m) \\
&= 256mn + 11774m + 258.
\end{aligned}$$

Theorem 3. Let H be a molecular graph of Camptothecin-Polymer Conjugate IT-101 structure, then ve-degree based indices of end vertices of each edges are given by,

(a) $M_1^{\beta ve}(H) = 80mn + 4441m + 105.$

(b) $M_2^{\beta ve}(H) = 256mn + 16160m + 306.$

Proof. According to definition of ve-degree of end vertices of each edge, we divides the edges into 46 partitions i.e., $E_1^*, E_2^*E_3^*, \ldots, E_{46}^*$ respectively, as shown in Table 3.

By using the table we can compute indices based on ve-degree of end vertices of each edge as **(a)** The first Zagreb β-index

$$\begin{aligned}
M_1^{\beta ve}(H) &= \sum_{uv\in E(H)} (\Lambda_{ve}(u) + \Lambda_{ve}(v)) \\
M_1^{\beta ve}(H) &= (7)|E_1^*| + (10)|E_2^*| + (11)|E_3^*| + (12)|E_4^*| + (10)|E_5^*| + (11)|E_6^*| + (12)|E_7^*| \\
&+ (13)|E_8^*| + (14)|E_9^*| + (15)|E_{10}^*| + (14)|E_{11}^*| + (14)|E_{12}^*| + (13)|E_{13}^*| + (16)|E_{14}^*| \\
&+ (14)|E_{15}^*| + (19)|E_{16}^*| + (16)|E_{17}^*| + (17)|E_{18}^*| + (19)|E_{19}^*| + (14)|E_{20}^*| + (15)|E_{21}^*| \\
&+ (16)|E_{22}^*| + (17)|E_{23}^*| + (16)|E_{24}^*| + (17)|E_{25}^*| + (18)|E_{26}^*| + (19)|E_{27}^*| + (20)|E_{28}^*| \\
&+ (15)|E_{29}^*| + (19)|E_{30}^*| + (16)|E_{31}^*| + (17)|E_{32}^*| + (18)|E_{33}^*| + (19)|E_{34}^*| + (15)|E_{35}^*| \\
&+ (20)|E_{36}^*| + (17)|E_{37}^*| + (22)|E_{38}^*| + (17)|E_{39}^*| + (16)|E_{40}^*| + (17)|E_{41}^*| + (19)|E_{42}^*| \\
&+ (22)|E_{43}^*| + (22)|E_{44}^*| + (20)|E_{45}^*| + (18)|E_{46}^*| \\
&= (7)(19m) + (10)(18m) + (11)(6m) + (12)(m+1) + (10)(6) + (11)(10m) \\
&+ (12)(4mn+30m) + (13)(11m) + (14)(4m) + (15)(30m) + (14)(4m) + (14)(4m) \\
&+ (13)(5m) + (16)(14m) + (14)(4m) + (19)(2m) + (16)(mn+7m) + (17)(14m) \\
&+ (19)(14m) + (14)(6m) + (15)(2m) + (16)(6m) + (17)(8m) + (16)(3m) + (17)(4m) \\
&+ (18)(2m) + (19)(2m) + (20)(2m) + (15)(2m) + (19)(2m) + (16)(2m) + (17)(m) \\
&+ (18)(4m) + (19)(3m) + (15)(m+1) + (20)(m) + (17)(2m) + (22)(2m) + (17)(2m) \\
&+ (16)(mn) + (17)(2m) + (19)(9m) + (22)(2m) + (22)(21m) + (20)(7m) + (18)(1) \\
&= 80mn + 4441m + 105.
\end{aligned}$$

(b) The second Zagreb β-index

$$\begin{aligned}
M_2^{\beta ve}(H) &= \sum_{uv\in E(H)} (\Lambda_{ve}(u) \times \Lambda_{ve}(v)) \\
M_2^{\beta ve}(H) &= (10)|E_1^*| + (21)|E_2^*| + (24)|E_3^*| + (27)|E_4^*| + (24)|E_5^*| + (28)|E_6^*| + (32)|E_7^*| \\
&+ (36)|E_8^*| + (40)|E_9^*| + (44)|E_{10}^*| + (48)|E_{11}^*| + (49)|E_{12}^*| + (40)|E_{13}^*| + (55)|E_{14}^*| \\
&+ (49)|E_{15}^*| + (84)|E_{16}^*| + (64)|E_{17}^*| + (72)|E_{18}^*| + (88)|E_{19}^*| + (49)|E_{20}^*| + (56)|E_{21}^*| \\
&+ (63)|E_{22}^*| + (70)|E_{23}^*| + (64)|E_{24}^*| + (72)|E_{25}^*| + (80)|E_{26}^*| + (90)|E_{27}^*| + (100)|E_{28}^*| \\
&+ (56)|E_{29}^*| + (84)|E_{30}^*| + (64)|E_{31}^*| + (72)|E_{32}^*| + (80)|E_{33}^*| + (88)|E_{34}^*| + (54)|E_{35}^*| \\
&+ (99)|E_{36}^*| + (70)|E_{37}^*| + (120)|E_{38}^*| + (70)|E_{39}^*| + (64)|E_{40}^*| + (72)|E_{41}^*| + (88)|E_{42}^*| \\
&+ (120)|E_{43}^*| + (121)|E_{44}^*| + (99)|E_{45}^*| + (81)|E_{46}^*| \\
&= (10)(19m) + (21)(18m) + (24)(6m) + (27)(m+1) + (24)(6) + (28)(10m) \\
&+ (32)(4mn+30m) + (36)(11m) + (40)(4m) + (44)(30m) + (48)(4m) + (49)(4m) \\
&+ (40)(5m) + (55)(14m) + (49)(4m) + (84)(2m) + (64)(mn+7m) + (72)(14m) \\
&+ (88)(7m) + (49)(6m) + (56)(2m) + (63)(6m) + (70)(8m) + (64)(3m) + (72)(4m) \\
&+ (80)(2m) + (90)(2m) + (100)(2m) + (56)(2m) + (84)(2m) + (64)(2m) + (72)(m) \\
&+ (80)(4m) + (88)(3m) + (54)(m+1) + (99)(m) + (70)(2m) + (120)(2m) \\
&+ (70)(2m) + (64)(mn) + (72)(2m) + (88)(9m) + (120)(2m) + (121)(21m) \\
&+ (99)(7m) + (81)(1) \\
&= 256mn + 16160m + 306.
\end{aligned}$$

Table 12 Numerical results of indices for Camptothecin-Polymer Conjugate IT-101.

$[m,n]$	$M^{ev}(H)$	$R^{ev}(H)$	$M_1^{\alpha ve}(H)$	$M_1^{\beta ve}(H)$	\color{black} {M}_{2}^{\beta ve}(H)
[1, 1]	10512	133.0960589	12288	4626	16722
[2, 2]	21160	267.3542194	24830	9307	33650
[3, 3]	32208	406.7136921	37884	14148	51090
[4, 4]	43656	551.1744769	51450	19149	69042
[5, 5]	55504	700.7365737	65528	24310	87506
[6, 6]	67752	855.3999827	80118	29631	106482
[7, 7]	80400	1015.164704	95220	35112	125970
[8, 8]	93448	1180.030738	110834	40753	145970
[9, 9]	106896	1349.998082	126960	46554	166482
[10, 10]	120744	1525.066740	143598	52515	187506

6. Numerical results

In this section, we will discuss the numerical results related to the eV-degree and ve-degree based topological descriptors for the Camptothecin-Polymer Conjugate IT-101 molecular structures. We have used different values of m and n and computed numerical values for the eV-degree and ve-degree based indices such as $M^{ev}(H), R^{ev}(H), M_1^{\alpha ve}(H), M_1^{\beta ve}(H)$ and $M_2^{\beta ve}(H)$ for the Camptothecin-Polymer Conjugate IT-101 structures. (see Table 11).

We can see in Table 12 and Figs. 13–15 that value topological descriptors increases when we increase the value of m and n. The Zagreb types indices were found to occur for the computation of the total π-electron energy of molecules; thus, for higher values of m and n, the total π-electron energy is increasing. The Randić index is used in the study of the chemical similarity of molecular compounds and in computing the Kovats constants and boiling point of molecules. The results shows

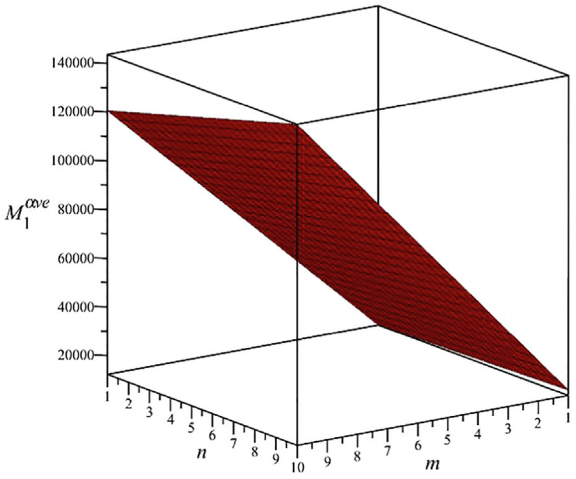

Fig. 14 The first Zagreb α-index.

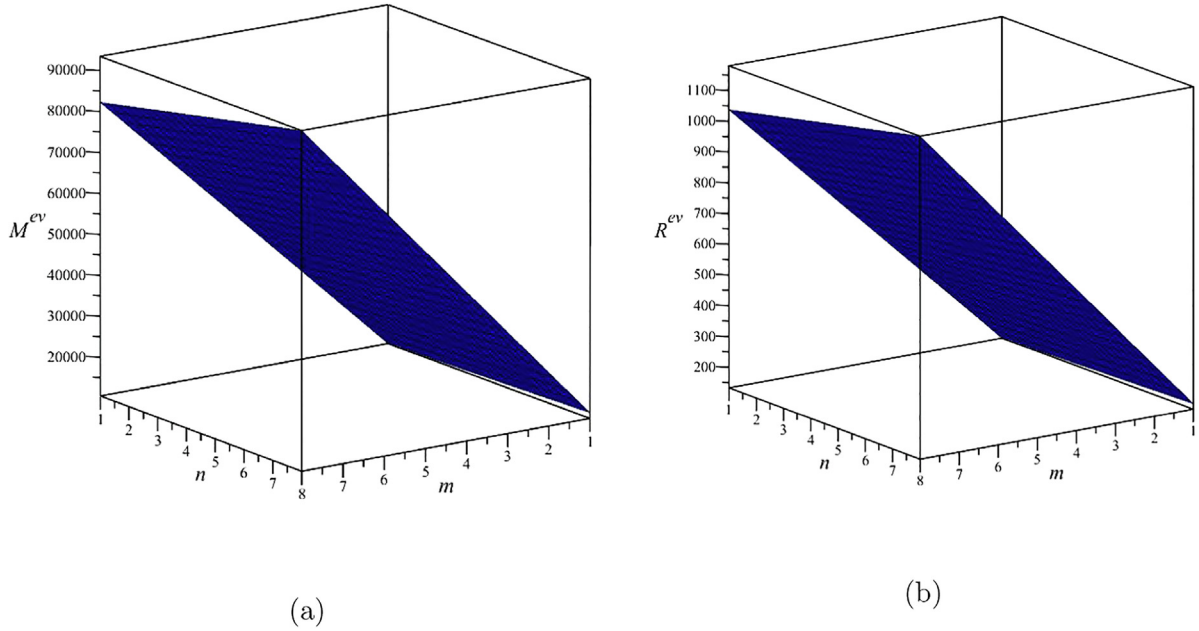

Fig. 13 The eV-degrees based indices, (a) The Zagreb index, (b) The Randic index.

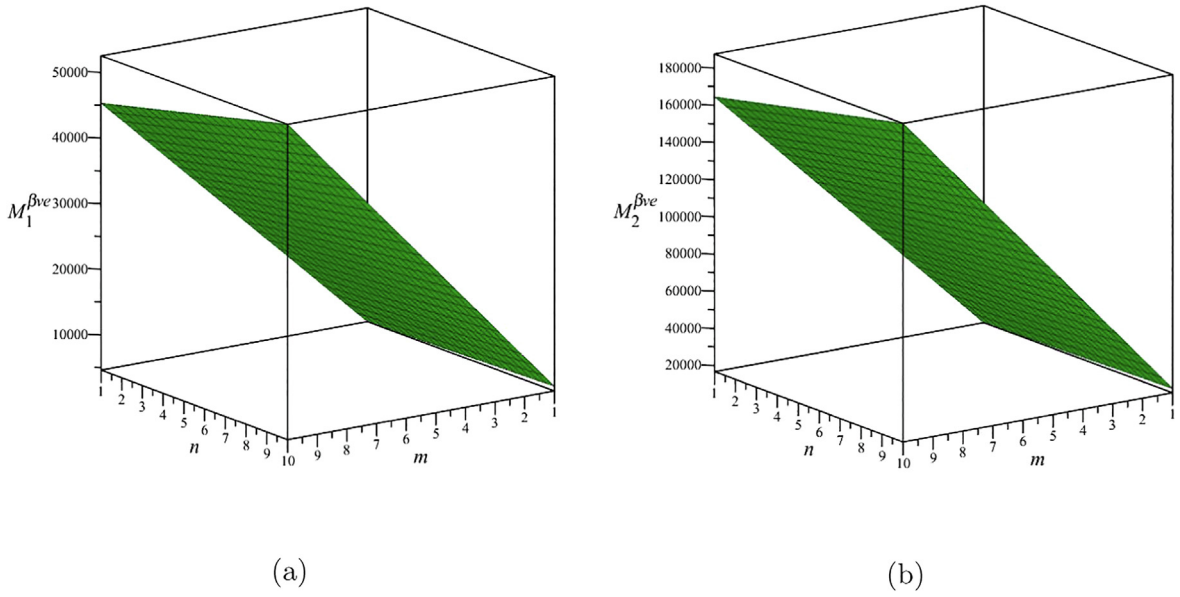

Fig. 15 (a) The first Zagreb β-index, (b) The second β-Zagreb index.

that the value of Randic index increases and with the increase in value of m and n.

7. Conclusion

We proposed topological indices based on eV-degree and ve-degree concepts. It has been shown that these indices can be used as predictive means in QSPR researches. The predictive power of these indices has been tested by using some physio-chemical properties of COVID drug-related compounds. Acquired results show that all the results are highly significant and there exists a strong positive linear bivariate relationship in the molecular weight, topological polar surface, and the used topological indices. But the indices cannot determine docking scores and binding affinity, and the results are insignificant for these chemical properties. The index $M_1^{\beta ve}$ is the best predictor of topological polar surface and molecular weight. $M_1^{\beta ve}$ has a high influence on topological polar surface and molecular weight. The observed values fall closer to the fitted line. Moreover, the ve-degree and eV-degree based topological indices of anti-tumor drug Camptothecin-Polymer Conjugate IT-101 have been calculated at the end.

Declaration of Competing Interest

None.

References

Al-Ahmadi, Bashair, Saleh, Anwar, Al-Shammakh, Wafa, 2021. Downhill Zagreb Topological Indices and M dn-Polynomial of Some Chemical Structures Applied for the Treatment of COVID-19 Patients. Open Journal of Applied Sciences 10 (04), 395.

Balaban, A.T., 1982. Highly discriminating distance-based topological index. Chemical physics letters 89 (5), 399–404.

Bollobás, B., Erdös, P., 1998. Graphs of extremal weights. Ars Combinatoria 50, 225–233.

Chellali, M., Haynes, T.W., Hedetniemi, S.T., Lewis, T.M., 2017. On ve-degrees and ev-degrees in graphs. Discrete Mathematics 340 (2), 31–38.

Chen, Shu-Bo, Rauf, Abdul, Ishtiaq, Muhammad, Naeem, Muhammad, Aslam, Adnan, 2021. On ve-degree-and ev-degree-based topological properties of crystallographic structure of cuprite Cu2O. Open Chemistry 19 (1), 576–585.

Estrada, E., Torres, L., Rodriguez, L., Gutman, I., 1998. Indian J. Chem. 37A, 849–855.

Ghosh, A.K., Xi, K., Ratia, K., Santarsiero, B.D., Fu, W., Harcourt, B.H., Rota, P.A., Baker, S.C., Johnson, M.E., Mesecar, A.D., 2005. Design and synthesis of peptidomimetic severe acute respiratory syndrome chymotrypsin-like protease inhibitors. Journal of medicinal chemistry 48 (22), 6767–6771.

Gutman, I., Trinajstic, N., 1972. Chem. Phys. Lett. 17, 535–538.

Hayat, Sakander, Khan, Suliman, 2021. Quality testing of spectrum-based valency descriptors for polycyclic aromatic hydrocarbons with applications. J. Mol. Struct. 1228, 129789.

Horoldagva, Batmend, 2019. Kinkar Ch Das, and Tsend-Ayush Selenge. On ve-degree and evdegree of graphs. Discrete Optimization 31, 1–7.

Hosamani, Sunilkumar M., Kulkarni, Bhagyashri B., Boli, Ratnamma G., Gadag, Vijay M., 2017. QSPR analysis of certain graph theocratical matrices and their corresponding energy. Applied Mathematics and Nonlinear Sciences 2 (1), 131–150.

Hosamani, Sunilkumar, Deepa Perigidad, S., Jamagoud, Y. Maled, Gavade, Sharada, 2017. QSPR analysis of certain degree based topological indices. J. Stat. Appl. Pro 6 (2), 361–371.

Ji, W., Wang, W., Zhao, X., Zai, J., Li, X., 2020. Cross-species transmission of the newly identified coronavirus 2019-nCoV. Journal of medical virology 92 (4), 433–440.

Kirmani, Syed Ajaz K., Parvez Ali, and Faizul Azam. Topological indices and QSPR/QSAR analysis of some antiviral drugs being investigated for the treatment of COVID-19 patients. International Journal of Quantum Chemistry 121, no. 9 (2021): e26594.

Kumar, V., Tan, K.P., Wang, Y.M., Lin, S.W., Liang, P.H., 2016. Identification, synthesis and evaluation of SARS-CoV and MERS-CoV 3C-like protease inhibitors. Bioorganic and medicinal chemistry 24 (13), 3035–3042.

Kumar, V., Tan, K.P., Wang, Y.M., Lin, S.W., Liang, P.H., 2016 Jul 1. Identification, synthesis and evaluation of SARS-CoV and

MERS-CoV 3C-like protease inhibitors. Bioorganic & medicinal chemistry. 24 (13), 3035–3042.

Yi-Xia Li, Abdul Rauf, Muhammad Naeem, Muhammad Ahsan Binyamin, Adnan Aslam, Valency-Based Topological Properties of Linear Hexagonal Chain and Hammer-Like Benzenoid, Complexity, vol. 2021, 2021.

Liu, L.F., Desai, S.D., LI, T.K., Mao, Y., Sun, M.E.I. and SIM, S.P., 2000. Mechanism of action of camptothecin. Annals of the New York Academy of Sciences, 922(1), pp.1-10.

Liu, Jia-Bao, Micheal Arockiaraj, M. Arulperumjothi, and Savari Prabhu. Distance based and bond additive topological indices of certain repurposed antiviral drug compounds tested for treating COVID-19. International Journal of Quantum Chemistry 121, no. 10 (2021): e26617.

Luccic, Bono, Lukovits, István, Nikolić, Sonja, Trinajstić, Nenad, 2001. Distance-related indexes in the quantitative structure- property relationship modeling. Journal of chemical information and computer sciences 41 (3), 527–535.

Mittal, L., Srivastava, M., Asthana, S., 2019. Conformational characterization of linker revealed the mechanism of cavity formation by 227G in BVDV RDRP. J. Phys. Chem. B 123 (29), 6150–6160.

Mondal, Sourav, De, Nilanjan, Pal, Anita, 2020. Topological indices of some chemical structures applied for the treatment of COVID-19 patients. Polycyclic Aromat. Compd., 1–15

Mondal, Sourav, Nilanjan De, Anita Pal, and Wei Gao. Molecular descriptors of some chemicals that prevent COVID-19. Current organic synthesis (2020).

Mondal, Sourav, Dey, Arindam, De, Nilanjan, Pal, Anita, 2021. QSPR analysis of some novel neighbourhood degree-based topological descriptors. Complex & Intelligent Systems 7 (2), 977–996.

Muralidharan, N., Sakthivel, R., Velmurugan, D., Gromiha, M.M., 2020. Computational studies of drug repurposing and synergism of lopinavir, oseltamivir and ritonavir binding with SARS-CoV-2 protease against COVID-19. J. Biomol. Struct. Dyn., 1–6

Nandini, G., Kirithiga, R. Sundara, Rajan, A. Arul, Shantrinal, T.M. Rajalaxmi, Rajasingh, Indra, Balasubramanian, Krishnan, 2020. Topological and Thermodynamic Entropy Measures for COVID-19 Pandemic through Graph Theory. Symmetry 12 (12), 1992.

Needle, D., Lountos, G.T., Waugh, D.S., 2015. Structures of the Middle East respiratory syndrome coronavirus 3C-like protease reveal insights into substrate specificity. Acta Crystallographica Section D: Biological Crystallography. 71 (5), 1102–1111.

Nutho, B., Mahalapbutr, P., Hengphasatporn, K., Pattaranggoon, N. C., Simanon, N., Shigeta, Y., Hannongbua, S., Rungrotmongkol, T., 2020. Why are lopinavir and ritonavir effective against the newly emerged Coronavirus 2019, Atomistic insights into the inhibitory mechanisms. Biochemistry 59 (18), 1769–1779.

Pant, S., Singh, M., Ravichandiran, V., Murty, U.S.N., Srivastava, H. K., 2020. Peptide- like and small-molecule inhibitors against Covid-19. J. Biomol. Struct. Dyn., 1–15

Pillaiyar, T., Manickam, M., Namasivayam, V., Hayashi, Y., Jung, S. H., 2016. An overview of severe acute respiratory syndrome-coronavirus (SARS-CoV) 3CL protease inhibitors: peptidomimetics and small molecule chemotherapy. Journal of medicinal chemistry 59 (14), 6595–6628.

Pushpakom, S., Iorio, F., Eyers, P.A., Escott, K.J., Hopper, S., Wells, A., Doig, A., Guilliams, T., Latimer, J., McNamee, C., Norris, A., Sanseau, P., Cavalla, D., Pirmohamed, M., 2019. Drug repurposing: Progress, challenges and recommendations. Nat. Rev. Drug Discovery 18 (1), 41–58.

Randic, M., 1975. Characterization of molecular branching. J. Am. Chem. Soc. 97 (23), 6609–6615.

Rauf, Abdul, Ishtiaq, Muhammad, Siddiqui, Muhammad Kamran, 2021. Topological study of hydroxychloroquine conjugated molecular structure used for novel coronavirus (COVID-19) treatment. Polycyclic Aromat. Compd., 1–17

Safa, Fariba, Yekta, Melody, 2017. Quantitative structure-property relationship study of standard formation enthalpies of acyclic alkanes using atom-type-based AI topological indices. Arabian Journal of Chemistry 10 (4), 439–447.

B. ŞAHIN1, AND S. EDIZ, On ev-Degree and ve-Degree Topological Indices, Iranian J. Math. Chem. 9 (4) December (2018) 263 - 277.

Sahoo, Sagarika, Patel, Sabita, Mishra, B.K., 2011. Quantitative structure property relationship for Henry's law constant of some alkane isomers. Thermochimica acta 512 (1–2), 273–277.

Saleh, Anwar, Sophia Shalini, G.B., Dhananjayamurthy, B.V., 2021. The Reduced Neighborhood Topological Indices and RNM-Polynomial for the Treatment of COVID-19. Biointerface Research in Applied Chemistry, 11817–11832.

Schluep, Thomas, Hwang, Jungyeong, Cheng, Jianjun, Heidel, Jeremy D., Bartlett, Derek W., Hollister, Beth, Davis, Mark E., 2006. Preclinical efficacy of the camptothecin-polymer conjugate IT-101 in multiple cancer models. Clin. Cancer Res. 12 (5), 1606–1614.

Schultz, A.G., 1973. Camptothecin. Chemical reviews 73 (4), 385–405.

Shao, Z., Wu, P., Zhang, X., Dimitrov, D., Liu, J.B., 2018. On the maximum ABC index of graphs with prescribed size and without pendent vertices. IEEE Access 6, 27604–27616.

Shirakol, Shailaja, Kalyanshetti, Manjula, Hosamani, Sunilkumar M., 2019. QSPR analysis of certain distance based topological indices. Applied Mathematics and Nonlinear Sciences 4 (2), 371–386.

Thomas, C.J., Rahier, N.J., Hecht, S.M., 2004. Camptothecin: current perspectives. Bioorganic and medicinal chemistry 12 (7), 1585–1604.

ul Qamar, Muhammad Tahir, Safar M. Alqahtani, Mubarak A. Alamri, and Ling-Ling Chen. Structural basis of SARS-CoV-2 3CLpro and anti-COVID-19 drug discovery from medicinal plants. Journal of pharmaceutical analysis 10, no. 4 (2020): 313-319.

Vukičević, B., Furtula, B., 2009. J. Math. Chem. 46, 1369–1376.

Wei, Jianxin, Murat Cancan, Atiq Ur Rehman, Muhammad Kamran Siddiqui, Muhammad Nasir, Muhammad Tayyab Younas, and Muhammad Farhan Hanif. On Topological Indices of Remdesivir Compound Used in Treatment of Corona Virus (COVID 19). Polycyclic Aromatic Compounds (2021): 1–19.

Wiener, H., 1947. Structural determination of paraffin boiling points. Journal of the American chemical society 69 (1), 17–20.

Xu, X., Chen, P., Wang, J., Feng, J., Zhou, H., Li, X., Zhong, W., Hao, P., 2020. Evolution of the novel coronavirus from the ongoing Wuhan outbreak and modeling of its spike protein for risk of human transmission. Science China Life Sciences 63 (3), 457–460.